◆ Human Brain Mapping 33:2499–2508 (2012) ◆

Modulating Cortico-Striatal and Thalamo-Cortical Functional Connectivity with Transcranial Direct Current Stimulation

Rafael Polanía*, Walter Paulus, and Michael A. Nitsche

Department of Clinical Neurophysiology, Georg-August University of Göttingen, 37075 Göttingen, Germany

Abstract: Transcranial direct current stimulation (tDCS) is a noninvasive brain stimulation technique that has been shown to alter cortical excitability and activity via application of weak direct currents. Beyond intracortical effects, functional imaging as well as behavioral studies are suggesting additional tDCS-driven alterations of subcortical areas, however, direct evidence for such effects is scarce. We aimed to investigate the impact of tDCS on cortico-subcortical functional networks by seed functional connectivity analysis of different striatal and thalamic regions to prove tDCS-induced alterations of the cortico-striato-thalamic circuit. fMRI resting state data sets were acquired immediately before and after 10 min of bipolar tDCS during rest, with the anode/cathode placed over the left primary motor cortex (M1) and the cathode/anode over the contralateral frontopolar cortex. To control for possible placebo effects, an additional sham stimulation session was carried out. Functional coupling between the left thalamus and the ipsilateral primary motor cortex (M1) significantly increased following anodal stimulation over M1. Additionally, functional connectivity between the left caudate nucleus and parietal association cortices was significantly strengthened. In contrast, cathodal tDCS over M1 decreased functional coupling between left M1 and contralateral putamen. In summary, in this study, we show for the first time that tDCS modulates functional connectivity of cortico-striatal and thalamo-cortical circuits. Here we highlight that anodal tDCS over M1 is capable of modulating elements of the cortico-striato-thalamo-cortical functional motor circuit. *Hum Brain Mapp 33:2499–2508, 2012.* © 2011 Wiley Periodicals, Inc.

Key words: tDCS; functional connectivity; plasticity; fMRI; stimulation; resting; subcortical; thalamus; striatum

INTRODUCTION

Transcranial direct current stimulation (tDCS) is a noninvasive brain stimulation technique, which has been shown to alter cortical excitability and activity via application of weak direct currents. Anodal tDCS over the motor cortex during rest increases and cathodal tDCS decreases cortical excitability [Nitsche and Paulus 2000, 2001; Nitsche et al., 2003b]. The after-effects of tDCS are NMDA receptor-dependent [Liebetanz et al., 2002; Nitsche et al., 2003a, 2004], and thus share some similarities with long term potentiation, and depression, which resemble well-known neuroplastic phenomena thought to underlie cognitive processes like learning and memory formation [Rioult-Pedotti et al., 2000]. In accordance, anodal tDCS of the

Additional Supporting Information may be found in the online version of this article.

Contract grant sponsor: The Rose Foundation.

*Correspondence to: Rafael Polanía, Department of Clinical Neurophysiology, Georg-August University of Göttingen, 37075 Göttingen, Robert Koch Str 40, Germany.
E-mail: rafael.polania@med.uni-goettingen.de

Received for publication 13 January 2011; Revised 19 April 2011; Accepted 18 May 2011

DOI: 10.1002/hbm.21380

Published online 16 September 2011 in Wiley Online Library (wileyonlinelibrary.com).

motor cortex improves motor learning and nondominant hand function in healthy subjects [Boggio et al., 2006; Nitsche et al., 2003c], as well as fine motor skills in stroke patients with respective deficits [Boggio et al., 2009b; Fregni et al., 2005; Hummel and Cohen 2005; Hummel et al., 2005]. These effects can be readily explained by the effect of tDCS on the primary motor cortex, and indeed it was demonstrated that tDCS modulates local intracortical circuits [Nitsche et al., 2005]. However, some other functional effects of tDCS are more compatible with an additional alteration of subcortical areas. tDCS over M1 induces changes in thermal and mechanical sensory percepts [Bachmann et al., 2010] and produces long lasting pain relief in chronic pain patients [Antal et al., 2010; Boggio et al., 2009a; Fenton et al., 2009; Williams et al., 2009]. These effects have been attributed to suppression of thalamic sensory pathways following motor cortex stimulation. Additionally, motor cortex tDCS improves gait and bradykinesia in patients suffering from Parkinson's disease (PD) [Benninger et al., 2010], which might be caused by tDCS-induced alterations of basal ganglia function. The results of these studies suggest that cortico-striato-thalamo-cortical circuits might be modulated by transcranial cortical stimulation. In principle accordance, a positron emission tomography (PET) study showed that tDCS over M1 induces widespread bidirectional changes in regional neuronal activities of cortical and subcortical regions, including striatal and thalamic areas [Lang et al., 2005]. However, this study does not allow drawing conclusions if the subcortical effects are connectivity-driven or caused by direct DC-induced effects on these areas. Evaluating the effects of tDCS on functional connectivity might help to clarify this question.

Functional connectivity analysis of resting state BOLD-fMRI fluctuations has enhanced our understanding of the human neural functional architecture in recent years [Cole et al., 2010]. Spontaneous cerebral activity measured by BOLD-fMRI shows consistent large-scale spatial patterns of coherent signals, which are compatible with both the underlying structural connectivity of the brain and the functional anatomy of the regions related to task performance [Beckmann et al., 2005; De Luca et al., 2006]. Hereby, a priori selection of a region of interest (ROI) allows identifying straightforward the functional architecture of a given cerebral area. In healthy subjects, it was shown that cortico-cortical functional networks are altered by tDCS, thus suggesting tDCS-induced cortico-cortical functional modulations [Polania et al., in press, 2011]. However, the impact of tDCS on cortico-subcortical functional circuits has been so far not been explored. In this study, we aimed to perform seed functional connectivity analysis to explore the impact of tDCS in the cortico-striato-thalamo-cortical functional circuit. Thus, a priori we selected ROIs belonging to striatal regions and the thalamus.

We hypothesized that anodal tDCS over M1 would increase the functional connectivity between striatal and thalamic regions and cortical regions associated with motor function. Additionally, since tDCS applied during rest over M1 has been shown to alter activities of widespread brain areas including the prefrontal cortex, associative areas of the parietal cortex, striatal, and thalamic areas [Lang et al., 2005], we hypothesized effects of tDCS might be reflected in cortico-subcortical functional connectivity alterations.

METHODS

Subjects

Fourteen healthy volunteers (8 women; mean age: 26 ± 4 years; age range: 21–40 years) were included in the study. Subjects were informed about all aspects of the experiments and all gave informed consent. None of the subjects suffered from any neurological or psychological disorder, had metallic implants/implanted electric devices, or took any medication regularly, or in the 2 weeks before participation in any of the experiments. All subjects were right-handed, according to the Edinburgh handedness inventory [Oldfield 1971]. The experiments conform to the Declaration of Helsinki, and the experimental protocol was approved by the Ethics Committee of the University of Göttingen.

Transcranial Direct Current Stimulation

Direct current was provided via a pair of square rubber electrodes (7 × 5 cm), The basic material of the rubber electrodes is silicon with some electrical conductive media in it (graphite-carbon) with a volume conductivity of 2.8 Ohm/cm. This leads to electrodes with a resistance of 50 Ohm. Each stimulation electrode wire was equipped with a 5 kOhm resistor near the electrode to avoid heating due to huge RF impulses during scanning. To suppress artefacts from outside the scanner room, further high frequency attenuators were inserted into the circuit path manufactured to be compatible with the MR-scanner environment (NeuroConn GmbH, Ilmenau, Germany). The electrodes were connected to a specially developed battery-driven stimulator outside the magnet room (NeuroConn GmbH, Ilmenau, Germany). To properly position the electrodes over the M1 of the subjects' head, the representational field of the right hand was determined using suprathreshold TMS [optimal M1 representation of the right first dorsal interosseous muscle (FDI) by single pulse TMS]. Before subjects entered the MR scanner, for anodal stimulation over M1, the anodal tDCS electrode was placed over the respective left M1 hand area and the cathode above the contralateral right orbit using conventional electrode cream (see Fig. 1). For cathodal stimulation over M1, the current flux was reversed. tDCS was applied for 10 min at 1 mA current intensity inside the MRI scanner. For sham stimulation sessions, the current was applied for 30 seconds at the beginning of the stimulation and then turned off (20 seconds linear down ramping until 0 mA was reached). Subjects are not able to distinguish between

real and sham stimulation using this procedure [Gandiga et al., 2006]. The rationale for applying excitatory/inhibitory anodal/cathodal tDCS of the dominant hemisphere is that functional connectivity of this hemisphere is expected to be larger than that of the nondominant one [Amunts et al., 2000]. Moreover, this electrode montage—anode over the M1 and cathode over the contralateral frontopolar cortex—has been shown to be the optimal montage to enhance excitability of the motor cortex [Moliadze et al., 2010; Nitsche and Paulus 2000].

Functional Magnetic Resonance Imaging

fMRI was conducted in a 3 Tesla scanner (Magnetom TIM Trio, Siemens Healthcare, Erlangen, Germany) using a standard eight-channel phased array head coil. Subjects were placed supine inside the magnet bore and wore headphones for noise protection. Vital functions were monitored throughout the experiment. Initially, anatomic images based on a T1-weighted 3D turbo fast low angle shot (FLASH) MRI sequence at 1 mm^3 isotropic resolution were recorded [repetition time (TR) = 2,250 ms, inversion time: 900 ms, echo time (TE) = 3.26 ms, flip angle: 9°]. For BOLD fMRI, a multislice T2*-sensitive gradient-echo echo-planar imaging (EPI) sequence (TR = 1,800 ms, TE = 30 ms, and flip angle 70°) at 3 × 3 mm^2 resolution was used. Twenty-nine consecutive sections at 3 mm thickness angulated in an axial-to-coronal orientation, covering the whole brain, were acquired. One hundred and seventy-five contiguous EPI volumes were acquired for each fMRI data set, that is, ~6 min resting fMRI. After the initial T1 dataset acquisition, two resting-state fMRI datasets were acquired immediately before and after the application of tDCS inside the MRI scanner (see Fig. 1 for further details). The tDCS electrodes were disconnected from the stimulator during fMRI acquisition. No distortion was seen in the images as reported previously [Polania et al., 2011]. fMRI images were acquired before and after but not during tDCS application. Subjects were asked to relax, keep their eyes closed and "not to think about anything in particular." Each subject underwent three sessions: anodal, cathodal, and sham stimulation; the order of sessions was interindividually randomized and the single sessions were separated at least 8 days from each other. To control for possible placebo effects, subjects were blinded for the stimulation conditions.

fMRI Preprocessing

All functional pre-processing steps were carried out with the FSL software package (http://www.fmrib.ox.ac.uk/fsl/). The first two volumes of each fMRI dataset were discarded to allow for magnetization equilibrium. Motion correction was applied using MCFLIRT and slice-timing correction using Fourier-space time-series phase shifting [Jenkinson et al., 2002]. Afterwards spatial smoothing was applied using a Gaussian kernel of FWHM 5 mm. Then, each subject's entire four-dimensional (4D) dataset was scaled by its global mean, that is, mean-based intensity normalization of all volumes by the same factor. Subsequently a temporal band-pass filter was applied: Gaussian-weighted least-squares straight line fitting and Gaussian low-pass temporal filtering HWHM 3 seconds. Registration of the high resolution T1 weighted images to the MNI152 template (Montreal Neurological Institute) with 2 mm^2 was performed using the FSL linear registration tool [Jenkinson et al., 2002] and further refined using FNIRT nonlinear registration. Movement in each cardinal direction (X, Y, and Z) and rotational movement around three axes (pitch, yaw, and roll) were calculated for each participant and visually inspected for movement-related artefacts.

Nuisance Signal Regression

To control for physiological processes and motion-related artefacts in the functional connectivity analysis [Kelly et al., 2009] we regressed the following nine signals from each subject's 4-D datasets: the six motion parameters, the nuisance parameters from the white matter (WM), cerebrospinal fluid (CSF), and the global signal. The regression of CSF and WM removes fluctuations unlikely to be involved in specific regional correlations. Additionally, the whole brain signal is thought to reflect a combination of physiological processes (such as cardiac and respiratory fluctuations) and scanner drift. Therefore, we included it as a nuisance signal to minimize the influence of such factors [Birn et al., 2006; Fox et al., 2005]. Correction for time series autocorrelation (prewhitening) was performed. The six motion parameters were generated by MCFLIRT. The global signal parameter was generated by averaging across all voxels within the brain. To generate the WM and CSF nuisance parameters we first segmented each subject's T1 weighted high-resolution image using the FAST segmentation program in FSL. The resulting segmented WM and CSF images were thresholded to ensure 90% tissue type probability. The thresholded masks were applied to each subject's time series and the mean time series was calculated by averaging across all voxels within the mask.

This nuisance signal regression procedure produced prewhitened, 4D residual datasets for each subject. Finally, a voxelwise scaling was performed on the 4D residuals, by dividing each voxel's time series by its SD. This step ensures that the functional connectivity calculations represent partial correlation rather than regression parameter estimates and removes potential between-condition differences in the magnitude of BOLD fluctuations [Sorg et al., 2007].

Seeds and Functional Connectivity

We conducted a probability-weighted seed-based functional connectivity analysis of the following subcortical regions: left/right nucleus accumbens, caudate nucleus,

putamen, and thalamus. The left/right hemispheric subcortical masks were created as defined by the Harvard-Oxford Structural Atlas, a validated probabilistic atlas included in FSL, which parcellates each hemisphere into anatomically distinct cortical and subcortical regions [Kennedy et al., 1998]. In this atlas every voxel is assigned a value that corresponds to its probability of belonging to a given parcellated region. To control for interindividual anatomical variability for each subcortical region, we used these probability values thresholded at 50% to weight each voxel's time series with that region. Mean time series were then extracted for each of the eight subcortical regions used in this study across all the probability-weighted time series within that region.

Afterwards, we performed eight separate multiple regression analyses in which we regressed the 4D functional datasets for each subject before and after each of the fMRI-tDCS sessions, using the FSL program FEAT. The analyses produced subject's level maps from each 4D dataset of all voxels that were positively and negatively correlated with a given subcortical brain region (first-level analysis).

Group-Level Statistical Analysis

For each subject, the six first-level analyses (pre- and post-tDCS* anodal, cathodal, and sham tDCS) were entered into a second-level fixed effects analysis to test for within subject effects of real stimulation compared with sham. For each of the three separate tDCS sessions we contrasted the activation maps after-against before-tDCS. We then contrasted each of the real tDCS sessions with the sham session, to quantify for each individual subject the activation changes specifically induced by tDCS. These calculations are resumed in the following equation:

$$(\mathrm{tDCS}_{\mathrm{AFTER}} - \mathrm{tDCS}_{\mathrm{BEFORE}}) - (\mathrm{Sham}_{\mathrm{AFTER}} - \mathrm{Sham}_{\mathrm{BEFORE}})$$

Thus, this second-level analysis results in statistical maps for each participant ($n = 14$), which reflect the effects of stimulation. The 14 statistical maps resulting from the second-level analysis are entered into the third-level mixed effects (ME) analysis, which in other words is the group average of the 14 statistical maps that were obtained in the second-level analysis. For these group-level analyses, mixed-effects Z (Gaussian T/F) statistic images were thresholded at the cluster level determined by $Z > 2.3$ and a corrected cluster significance threshold of $P < 0.05$. By performing a second-level fixed effects analysis and a subsequent third-level ME analysis we were able to take into account both differences in variance between the two scans performed on the same day (after-before) as well as differences across fMRI sessions performed on different days (anodal, cathodal, and sham). A single second-level analysis would have been inappropriate, as equal variance between scans would have been assumed.

Finally, we investigated whether we were able to replicate the results of recent studies were probability-weighted ROIs of the striatum have been used [Di Martino et al., 2008; Kelly et al., 2009]. To this end, in a second-level analysis, we combined all three before stimulation fMRI scans of each subject (anodal, cathodal, and sham), and then we performed a third-level analysis between subjects to obtain patterns of functional connectivity for each seed ROI used in this study. For these group-level analyses, mixed-effects Z (Gaussian T/F) statistic images were thresholded at the cluster level determined by $Z > 2.3$ and a corrected cluster significance threshold of $P < 0.05$.

RESULTS

Movement and Post-Session Questionary

For each subject, the root mean square (rms) of the movement parameters did not exceed 1 mm or 1° in any of the cardinal directions or rotational axes. After each of the sessions, we asked the subjects whether they felt the stimulation. All participants in all sessions reported an itching, which completely disappeared few seconds after stimulation onset. Thus, participants were not able to discriminate between real and sham stimulation. Notice that for sham stimulation, the current was applied for 30 seconds and then turned off (20 seconds linear down ramping until 0 mA was reached). Subjects are not able to distinguish between real and sham stimulation using this procedure (see Methods) [Gandinga et al., 2006].

Striatal and Thalamic Functional Connectivity

Relative to previous studies the data in this study were acquired in a different magnet of different field strength [Di Martino et al., 2008; Kelly et al., 2009]. However, when using the before stimulation conditions our results show patterns of functional connectivity, which are consistent with those previously reported (Supporting Information).

Anodal tDCS over M1

The third level ME analysis showed that functional connectivity significantly increased between: (1) left thalamus and left precentral gyrus [Brodmann area (BA) 4; peak Z-value = 3.03, MNI $x = -62$, $y = -8$, $z = 26$; cluster size = 206 voxels] (see Fig. 2); and (2) between left caudate nucleus and superior parietal lobule (BA 7; peak Z-value = 3.12, MNI $x = -24$, $y = -62$, $z = 60$; cluster size = 228 voxels; see Fig. 3). Additionally, we found that functional connectivity between the left caudate nucleus and the posterior cingulate cortex, PCC, (peak Z-value = 2.91, MNI $x = -10$, $y = -58$, $z = 16$; cluster size = 223 voxels) was significantly decreased (see Fig. 4).

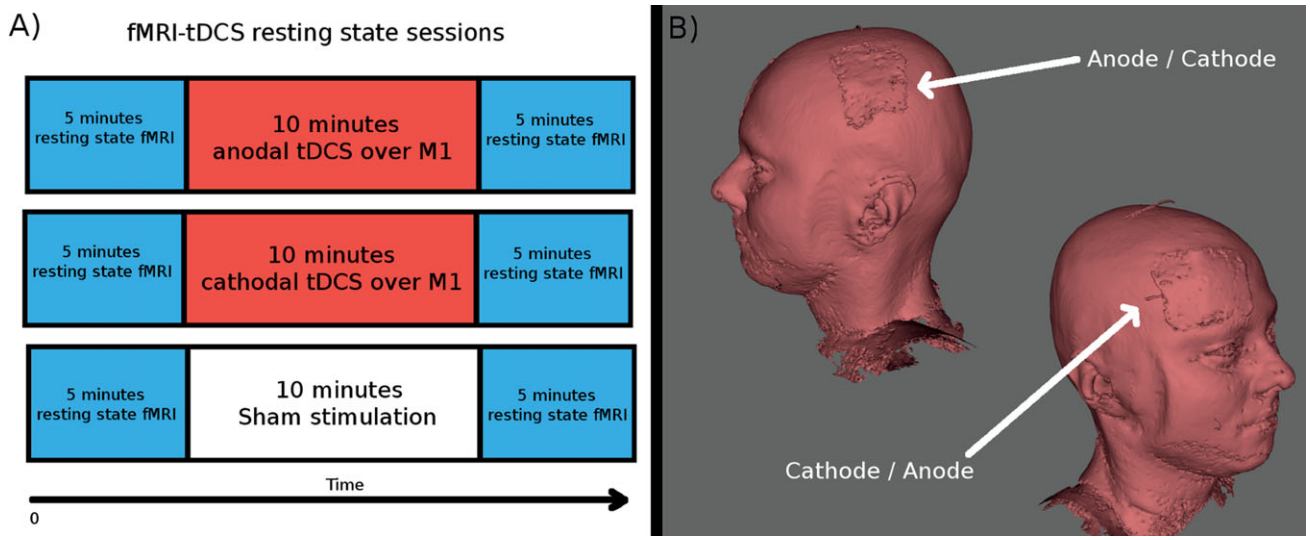

Figure 1.

(**A**) Shown is the experimental procedure. First 5 min resting state fMRI was acquired. Then 10 min tDCS was applied inside the MR scanner. Immediately afterwards, a new 5 min resting state fMRI was acquired. Each subject underwent three sessions: anodal tDCS over M1 (combined with cathodal tDCS over the contralateral frontopolar cortex), cathodal tDCS over M1 (combined with anodal tDCS over the contralateral frontopolar cortex) and sham stimulation. The order of sessions was interindividually randomized and the single sessions were separated by at least 8 days from each other. **(B)** A 3-dimensional reconstruction of the T1 image from one of the subjects is shown to illustrate the location of the electrodes. For anodal stimulation over M1 the anode was placed over the left M1 and the cathode over the contralateral frontopolar cortex. For cathodal stimulation over M1 the current flux was reversed. tDCS was applied inside the MR scanner, but not during EPI fMRI acquisition.

Cathodal tDCS over M1

The third level ME analysis showed that functional connectivity significantly decreased between the right putamen and the left precentral gyrus (BA 4; peak Z-value = 3.4, MNI $x = -60$, $y = -2$, $z = 14$; cluster size = 156 voxels; see Fig. 5). Additionally, we found that functional

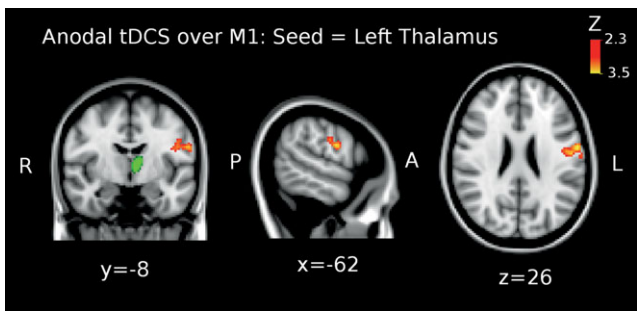

Figure 2.

Shown is the result of the third-level mixed effects (ME) analysis (see Methods) when using the left thalamus as seed (green colored region in the brain) for the functional connectivity analysis when anodal tDCS was applied over M1. Functional connectivity significantly increased between left thalamus and left precentral gyrus (Brodmann area (BA) 4; peak Z-value = 3.03, MNI $x = -62$, $y = -8$, $z = 26$; cluster size = 206 voxels). Images are displayed according to radiological convention (left is right).

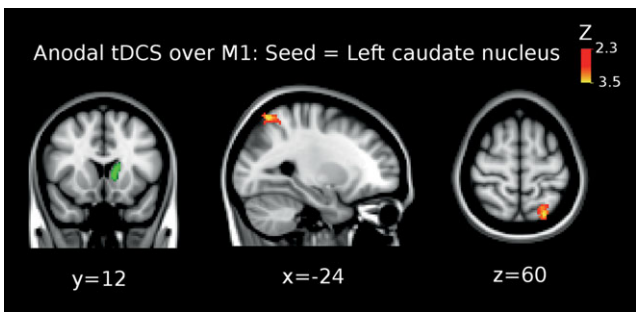

Figure 3.

Shown is the result of the third-level mixed effects (ME) analysis (see Methods) when using the left caudate nucleus as seed (green colored region in the brain) for the functional connectivity analysis when anodal tDCS was applied over M1. Functional connectivity significantly increased between left caudate nucleus and left superior parietal lobule (Brodmann area 7; peak Z-value = 3.12, MNI $x = -24$, $y = -62$, $z = 60$; cluster size = 228 voxels). Images are displayed according to radiological convention (left is right).

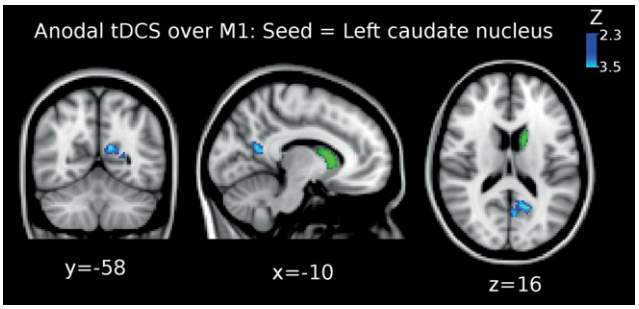

Figure 4.
Shown is the result of the third-level mixed effects (ME) analysis (see Methods) when using the left caudate nucleus as seed (green colored region in the brain) for the functional connectivity analysis when anodal tDCS was applied over M1. Functional connectivity significantly decreased between left caudate nucleus and posterior cingulate cortex (PCC) (peak Z-value = 2.91, MNI $x = -10$, $y = -58$, $z = 16$; cluster size = 223 voxels). Images are displayed according to radiological convention (left is right).

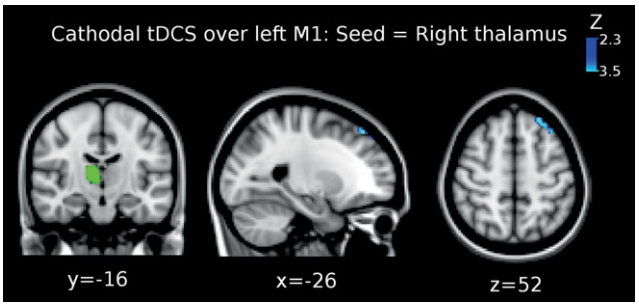

Figure 6.
Shown is the result of the third-level mixed effects (ME) analysis (see Methods) when using the right thalamus as seed (green colored region in the brain) for the functional connectivity analysis when cathodal tDCS was applied over M1. Functional connectivity significantly decreased between right thalamus and left superior frontal gyrus (peak Z-value = 3.3, MNI $x = -26$, $y = 36$, $z = 52$; cluster size = 206 voxels). Images are displayed according to radiological convention (left is right).

coupling between the right thalamus and the left superior frontal gyrus significantly decreased (peak Z-value = 3.3, MNI $x = -26$, $y = 36$, $z = 52$; cluster size = 206 voxels; see Fig. 6).

Iterative Connectivity Analysis

To further explore the increase in functional coupling between the left thalamus and the left motor cortex following anodal tDCS over M1, we performed an additional functional connectivity analysis taking as seed the left M1 cluster that showed a significant increase of functional connectivity with the left thalamus (see Fig. 2). The results of this iterative analysis support our primary findings showing that the functional coupling between the left M1 and left thalamus significantly increased (peak Z-value = 2.9; MNI $x = -10$, $y = -16$, $z = 14$; cluster size = 112 voxels; see Fig. 7). A second cluster showed significantly increased functional coupling between left M1, left thalamus and left caudate nucleus (peak Z-value = 3.2; MNI $x = -6$, $y = -4$, $z = 10$; cluster size = 150 voxels). Additionally, a cluster representing the primary somatosensory cortex showed significantly decreased functional coupling with the left M1 cluster (BA 2; peak Z-value = 3.51, MNI $x = -58$, $y = -18$, $z = 3$; cluster size = 351 voxels; see Fig. 8).

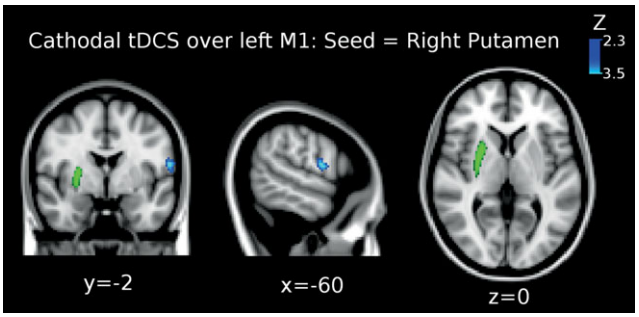

Figure 5.
Shown is the result of the third-level mixed effects (ME) analysis (see Methods) when using the right putamen (green colored region in the brain) for the functional connectivity analysis when cathodal tDCS was applied over M1. Functional connectivity significantly decreased between right putamen and left precentral gyrus (Brodmann area 4; peak Z-value = 3.4, MNI $x = -60$, $y = -2$, $z = 14$; cluster size = 156 voxels). Images are displayed according to radiological convention (left is right).

DISCUSSION

This work is the first resting state fMRI study to examine the effects of transcranial electric stimulation within cortico-subcortical functional networks. In line with our hypothesis, anodal tDCS over left M1 enhanced functional connectivity between the left primary motor cortex and the ipsilateral thalamus. This finding was further confirmed by an iterative functional connectivity analysis using the left M1 as seed region, where, additionally, we found an increase of functional connectivity of the left M1 with the ipsilateral caudate nucleus. Additionally, functional connectivity of the caudate nucleus, which receives afferents from the cortex and the thalamus, with associative areas such as the superior parietal cortex was enhanced. In contrast, functional coupling between the caudate nucleus and regions of the "default mode" network, particularly the PCC, was reduced. However, cathodal stimulation over left M1 combined with anodal simulation over the contralateral frontopolar cortex

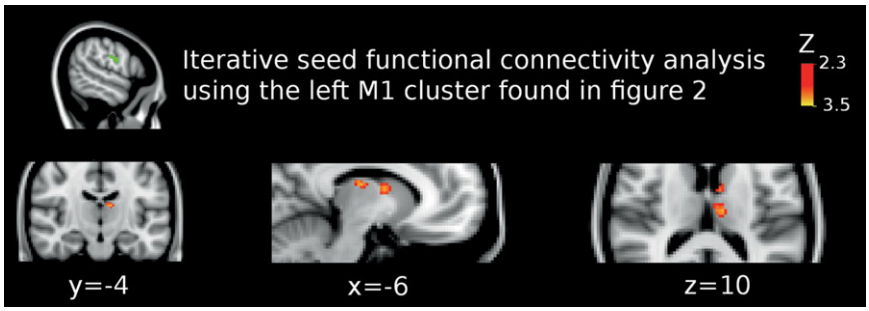

Figure 7.

Shown is the result of the iterative functional connectivity analysis using the left M1 cluster as seed (green colored region). In Figure 2, it is shown that this cluster enhanced functional coupling with the left thalamus (see figure 2) when anodal tDCS was applied over M1. Here, it is shown that functional connectivity significantly increased between left thalamus and left precentral gyrus (peak Z-value = 2.9; MNI $x = -10$, $y = -16$, $z = 14$; cluster size = 112 voxels). We found a second cluster that significantly increased functional coupling with the left M1, which represents the left thalamus and left caudate nucleus (peak Z-value = 3.2; MNI $x = -6$, $y = -4$, $z = 10$; cluster size = 150 voxels). Images are displayed according to radiological convention (left is right).

decreased functional coupling between the right putamen and the contralateral motor cortex. Additionally, in this stimulation condition the functional coupling of the right thalamus with the contralateral superior frontal gyrus was reduced.

Anodal tDCS Over M1

The application of anodal stimulation over M1 combined with the application of cathodal stimulation over the contralateral frontopolar cortex induced a remarkable increase of the functional coupling between the left thalamus and the ipsilateral motor cortex. This result is of great interest considering that anodal stimulation over the motor cortex has been shown to improve gait and bradykinesia in patients suffering from PD [Benninger et al., 2010]. In that study, Benninger et al., [2010] speculated whether thalamic activity could be theoretically modulated by cortical stimulation. Our results suggest that there seems to be a connectivity-driven alteration of thalamic activity caused by tDCS, being in favor for connectivity-driven indirect effects of tDCS on thalamic function. In fact, our iterative seed functional connectivity analysis (using the M1 region found in the initial analysis as seed, Figs. 2 and 7), showed specific locations of the thalamus and striatum (specifically the caudate nucleus) that were modulated by anodal stimulation of M1, thus delivering evidence that anodal stimulation over M1 modulates elements of the cortico-striato-thalamo-cortical functional motor circuit. It should be noticed however that the thalamic region showing up in Figure 7 belongs to a medial dorsal region, which has major connections with the prefrontal cortex (consider that major direct connections between thalamus and M1 origin primarily in ventro-medial and lateral thalamic regions). This may be explained by a tDCS-generated increase of cortico-cortical coupling between motor related and prefrontal areas, as revealed by graph theoretical analysis [Polania et al., 2011]. In addition, the relatively large size of the electrodes used in this study might have contributed to nonfocal effects [Nitsche et al., 2007]. This might be explored in future studies by reducing the size the effective stimulating electrode [Nitsche et al., 2007].

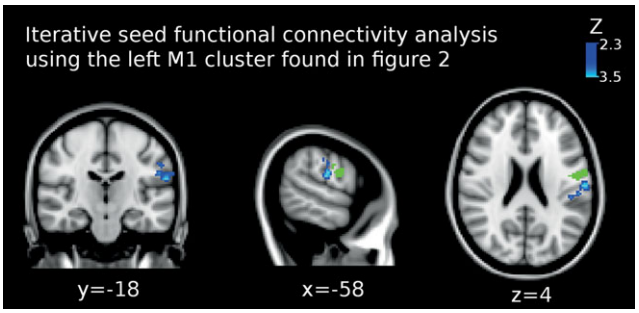

Figure 8.

Shown is the result of the iterative functional connectivity analysis using the left M1 cluster as seed (green colored region). In Figure 2, it is shown that this cluster enhanced the functional coupling with the left thalamus (see Fig. 2) when anodal tDCS was applied over M1. Functional connectivity significantly decreased between left M1 and left primary somatosensory cortex (Brodmann area 2; peak Z-value = 3.51, MNI $x = -58$, $y = -18$, $z = 3$; cluster size = 351 voxels). Images are displayed according to radiological convention (left is right).

In addition to the thalamic-M1 functional connectivity increase, we found that functional connectivity between the left caudate nucleus and the default mode network (i.e., the PCC) decreased. This was accompanied by an increase of functional connectivity between the left caudate

nucleus and the superior parietal cortex, which is an area activated during visuo-motor integration (e.g., reaching to grasp an object [Reichenbach et al., 2010]). Thus, it might be speculated that default resting network connectivity is reduced because the motor-related loop is activated by tDCS, which might mean a modulation ("switch") of activation patterns. This argument is supported by previous studies which have shown that activity and connectivity within the default mode network is reduced during task performance [Fransson 2006; McKiernan et al., 2003]. This effect is associated with increased activation in task-relevant regions [Tomasi et al., 2006].

Moreover, the iterative functional connectivity analysis using M1 as seed showed a significant decrease in the functional coupling between left M1 and the ipsilateral somatosensory (S1) cortex (see Fig. 8). The present fMRI-BOLD analysis allows to conclude that this "disconnection" is cortico-cortical and not due to thalamic-mediated effects, because we did not observe a reduced connectivity between the thalamus and S1. In principle, sensory perception could have altered functional connectivity, but that this is unlikely, because subjects did not report different perceptions between stimulation conditions, and MRI was conducted after tDCS, when no perceptions were present (see Methods and Results section). Recent studies have provided clear evidence that tDCS can reduce pain and chronic pain [Antal et al., 2010; Bachmann et al., 2010; O'Connell et al., 2010; Zaghi et al., 2009] and interestingly, in another recent study, anodal stimulation over M1 increased pain perception threshold for up to 6.5% in healthy volunteers [Boggio et al., 2008]. In this study, the investigators suggested that modulation of M1 with tDCS results in inhibition of thalamic activity, causing a decrease of thalamic hyperactivity that underlies chronic pain.

Cathodal tDCS Over M1

Application of cathodal tDCS over M1 combined with anodal tDCS over the contralateral frontopolar cortex did not result in any enhancement of functional connectivity between striatal or thalamic and any other brain regions. In contrast, we found a couple of regions where functional connectivity significantly decreased: (1) between the right putamen and the left M1 and (2) between the right thalamus and the left superior frontal gyrus. One reason why tDCS in the resting M1 did not induce antagonistic effects to anodal tDCS is that the effects of tDCS may depend on the background level of activity, that is, there is not much room for diminishing activity by cathodal tDCS if the level of cortico-subcortical activity during rest is low [Matsunaga et al., 2004]. Therefore, we hypothesize that cathodal tDCS over M1 might produce its effects in conditions with high levels of cortico-subcortical activity. Further experiments are required to address this point.

Interestingly, in both subcortical regions the decrease in functional coupling was observed in contralateral regions, contrary to what we observed with the application of anodal stimulation. This phenomenon might correlate with the results of a PET-tDCS study where Lang et al. [2005], using the same tDCS electrode montage, found that anodal tDCS over M1 induced more widespread increases in regional cerebral blood flow (rCBF) whereas cathodal tDCS decreased it. Additionally, it should be noticed that these structures (right putamen and left precentral gyrus, Fig. 5; right thalamus and left superior frontal gyrus, Fig. 6) have no monosynaptic anatomical connections, and it is even more intriguing that a mediating structure, which could cause reduced functional connectivity, was not identified in the analysis. One possible explanation for this result is based on the fact that in this study we used a bipolar cephalic electrode montage (anodal and cathodal electrodes with same size), and thus in case of cathodal stimulation of the primary motor cortex the excitability of the contralateral frontopolar cortex will be enhanced by simultaneous anodal stimulation. Therefore, it can be speculated that the excitability enhancement of the frontopolar cortex generated by anodal stimulation induced functional activity changes in connected ipsilateral subcortical structures, such as the putamen and thalamus, which in concert with the cathodal tDCS-induced excitability reduction of the contralateral frontal cortex might result in a desynchronization of these areas with respect to resting state activity without stimulation. The problem of parallel stimulation of two brain regions should be overcome in future studies by using other electrode montages, for example, by increasing the size of the reference electrode, making it functionally ineffective [Nitsche et al., 2007]. Another option might be to locate the reference electrode in an extracephalic region [Vandermeeren et al., 2010], however, it has been recently demonstrated that the distance of the reference electrode plays a crucial role in the induction of tDCS after-effects and also that the electrode montage used in this study—anode over the M1 and cathode over the contralateral frontopolar cortex—might be the optimal montage to enhance excitability of the motor cortex [Moliadze et al., 2010; Nitsche and Paulus 2000].

CONCLUSIONS AND FUTURE WORK

In summary, in this study, we show for the first time that tDCS modulates the functional connectivity of cortico-striatal and thalamo-cortical circuits. Here, we highlight that anodal tDCS over M1 combined with cathodal stimulation over the contralateral frontopolar cortex is capable of modulating elements of, among others, the cortico-striato-thalamo-cortical functional motor circuit by increasing the functional coupling of motor related areas with subcortical regions, and that this is accompanied by a reduction of the functional coupling between the striatum and the default mode network. Future studies should combine tDCS with task-related paradigms to learn more about the mechanisms of stimulation-induced functional cortico-subcortical and cortico-cortical modulations.

ACKNOWLEDGMENTS

The authors would like to express their gratitude to the Rose Foundation. Their support made possible to conduct this study, which they believe will help them to understand better the effects of tDCS in multiple sclerosis.

REFERENCES

Amunts K, Jancke L, Mohlberg H, Steinmetz H, Zilles K (2000): Interhemispheric asymmetry of the human motor cortex related to handedness and gender. Neuropsychologia 38:304–312.

Antal A, Terney D, Kuhnl S, Paulus W (2010): Anodal transcranial direct current stimulation of the motor cortex ameliorates chronic pain and reduces short intracortical inhibition. J Pain Symptom Manage 39:890–903.

Bachmann CG, Muschinsky S, Nitsche MA, Rolke R, Magerl W, Treede RD, Paulus W, Happe S (2010): Transcranial direct current stimulation of the motor cortex induces distinct changes in thermal and mechanical sensory percepts. Clin Neurophysiol 121:2083–2089.

Beckmann CF, DeLuca M, Devlin JT, Smith SM (2005): Investigations into resting-state connectivity using independent component analysis. Philos Trans R Soc Lond B Biol Sci 360:1001–1013.

Benninger DH, Lomarev M, Lopez G, Wassermann EM, Li X, Considine E, Hallett M (2010): Transcranial direct current stimulation for the treatment of Parkinson's disease. J Neurol Neurosurg Psychiatry 81:1105–1111.

Birn RM, Diamond JB, Smith MA, Bandettini PA (2006): Separating respiratory-variation-related fluctuations from neuronal-activity-related fluctuations in fMRI. Neuroimage 31:1536–1548.

Boggio PS, Castro LO, Savagim EA, Braite R, Cruz VC, Rocha RR, Rigonatti SP, Silva MT, Fregni F (2006): Enhancement of non-dominant hand motor function by anodal transcranial direct current stimulation. Neurosci Lett 404:232–236.

Boggio PS, Zaghi S, Lopes M, Fregni F (2008): Modulatory effects of anodal transcranial direct current stimulation on perception and pain thresholds in healthy volunteers. Eur J Neurol 15:1124–1130.

Boggio PS, Amancio EJ, Correa CF, Cecilio S, Valasek C, Bajwa Z, Freedman SD, Pascual-Leone A, Edwards DJ, Fregni F (2009a) Transcranial DC stimulation coupled with TENS for the treatment of chronic pain: A preliminary study. Clin J Pain 25:691–695.

Boggio PS, Zaghi S, Fregni F (2009b) Modulation of emotions associated with images of human pain using anodal transcranial direct current stimulation (tDCS). Neuropsychologia 47: 212–217.

Cole DM, Smith SM, Beckmann CF (2010): Advances and pitfalls in the analysis and interpretation of resting-state FMRI data. Front Syst Neurosci 4:8.

De Luca M, Beckmann CF, De Stefano N, Matthews PM, Smith SM (2006): fMRI resting state networks define distinct modes of long-distance interactions in the human brain. Neuroimage 29:1359–1367.

Di Martino A, Scheres A, Margulies DS, Kelly AM, Uddin LQ, Shehzad Z, Biswal B, Walters JR, Castellanos FX, Milham MP (2008): Functional connectivity of human striatum: A resting state FMRI study. Cereb Cortex 18:2735–2747.

Fenton BW, Palmieri PA, Boggio P, Fanning J, Fregni F (2009): A preliminary study of transcranial direct current stimulation for the treatment of refractory chronic pelvic pain. Brain Stimul 2:103–107.

Fox MD, Snyder AZ, Vincent JL, Corbetta M, Van Essen DC, Raichle ME (2005): The human brain is intrinsically organized into dynamic, anticorrelated functional networks. Proc Natl Acad Sci U S A 102:9673–9678.

Fransson P (2006): How default is the default mode of brain function? Further evidence from intrinsic BOLD signal fluctuations. Neuropsychologia 44:2836–2845.

Fregni F, Boggio PS, Mansur CG, Wagner T, Ferreira MJ, Lima MC, Rigonatti SP, Marcolin MA, Freedman SD, Nitsche MA, Pascual-Leone A (2005): Transcranial direct current stimulation of the unaffected hemisphere in stroke patients. Neuroreport 16:1551–1555.

Gandiga PC, Hummel FC, Cohen LG (2006): Transcranial DC stimulation (tDCS): A tool for double-blind sham-controlled clinical studies in brain stimulation. Clin Neurophysiol 117: 845–850.

Hummel F, Cohen LG (2005): Improvement of motor function with noninvasive cortical stimulation in a patient with chronic stroke. Neurorehabil Neural Repair 19:14–19.

Hummel F, Celnik P, Giraux P, Floel A, Wu WH, Gerloff C, Cohen LG (2005): Effects of non-invasive cortical stimulation on skilled motor function in chronic stroke. Brain 128(Pt 3):490–499.

Jenkinson M, Bannister P, Brady M, Smith S (2002): Improved optimization for the robust and accurate linear registration and motion correction of brain images. Neuroimage 17:825–841.

Kelly C, de Zubicaray G, Di Martino A, Copland DA, Reiss PT, Klein DF, Castellanos FX, Milham MP, McMahon K (2009): L-dopa modulates functional connectivity in striatal cognitive and motor networks: A double-blind placebo-controlled study. J Neurosci 29:7364–7378.

Kennedy DN, Lange N, Makris N, Bates J, Meyer J, Caviness VS Jr. (1998): Gyri of the human neocortex: An MRI-based analysis of volume and variance. Cereb Cortex 8:372–384.

Lang N, Siebner HR, Ward NS, Lee L, Nitsche MA, Paulus W, Rothwell JC, Lemon RN, Frackowiak RS (2005): How does transcranial DC stimulation of the primary motor cortex alter regional neuronal activity in the human brain? Eur J Neurosci 22:495–504.

Liebetanz D, Nitsche MA, Tergau F, Paulus W (2002): Pharmacological approach to the mechanisms of transcranial DC-stimulation-induced after-effects of human motor cortex excitability. Brain 125(Pt 10):2238–2247.

Matsunaga K, Nitsche MA, Tsuji S, Rothwell JC (2004): Effect of transcranial DC sensorimotor cortex stimulation on somatosensory evoked potentials in humans. Clin Neurophysiol 115: 456–460.

McKiernan KA, Kaufman JN, Kucera-Thompson J, Binder JR (2003): A parametric manipulation of factors affecting task-induced deactivation in functional neuroimaging. J Cogn Neurosci 15:394–408.

Moliadze V, Antal A, Paulus W (2010: Electrode-distance dependent after-effects of transcranial direct and random noise stimulation with extracephalic reference electrodes. Clin Neurophysiol 121:2165–2171.

Nitsche MA, Paulus W (2000): Excitability changes induced in the human motor cortex by weak transcranial direct current stimulation. J Physiol 527(Pt 3):633–639.

Nitsche MA, Paulus W (2001): Sustained excitability elevations induced by transcranial DC motor cortex stimulation in humans. Neurology 57:1899–1901.

Nitsche MA, Fricke K, Henschke U, Schlitterlau A, Liebetanz D, Lang N, Henning S, Tergau F, Paulus W (2003a): Pharmacological modulation of cortical excitability shifts induced by transcranial direct current stimulation in humans. J Physiol 553(Pt 1):293–301.

Nitsche MA, Nitsche MS, Klein CC, Tergau F, Rothwell JC, Paulus W (2003b) Level of action of cathodal DC polarisation induced inhibition of the human motor cortex. Clin Neurophysiol 114:600–604.

Nitsche MA, Schauenburg A, Lang N, Liebetanz D, Exner C, Paulus W, Tergau F (2003c) Facilitation of implicit motor learning by weak transcranial direct current stimulation of the primary motor cortex in the human. J Cogn Neurosci 15:619–626.

Nitsche MA, Liebetanz D, Schlitterlau A, Henschke U, Fricke K, Frommann K, Lang N, Henning S, Paulus W, Tergau F (2004): GABAergic modulation of DC stimulation-induced motor cortex excitability shifts in humans. Eur J Neurosci 19:2720–2726.

Nitsche MA, Seeber A, Frommann K, Klein CC, Rochford C, Nitsche MS, Fricke K, Liebetanz D, Lang N, Antal A, Paulus W, Tergau F (2005): Modulating parameters of excitability during and after transcranial direct current stimulation of the human motor cortex. J Physiol 568 (Pt 1):291–303.

Nitsche MA, Doemkes S, Karakose T, Antal A, Liebetanz D, Lang N, Tergau F, Paulus W (2007): Shaping the effects of transcranial direct current stimulation of the human motor cortex. J Neurophysiol 97:3109–3117.

O'Connell NE, Wand BM, Marston L, Spencer S, Desouza LH (2010): Non-invasive brain stimulation techniques for chronic pain. Cochrane Database Syst Rev 9:CD008208.

Oldfield RC (1971): The assessment and analysis of handedness: The Edinburgh inventory. Neuropsychologia 9:97–113.

Polania R, Nitsche MA, Paulus W: Modulating functional connectivity patterns and topological functional organization of the human brain with transcranial direct current stimulation. Hum Brain Mapp (in press). DOI: 10.1002/hbm. 21104.

Polania R, Paulus W, Antal A, Nitsche MA (2011): Introducing graph theory to track for neuroplastic alterations in the resting human brain: A transcranial direct current stimulation study. Neuroimage 54:2287–2296.

Reichenbach A, Bresciani JP, Peer A, Bulthoff HH, Thielscher A: Contributions of the PPC to Online Control of Visually Guided Reaching Movements Assessed with fMRI-Guided TMS. Cereb Cortex (in press).

Rioult-Pedotti MS, Friedman D, Donoghue JP (2000): Learning-induced LTP in neocortex. Science 290:533–536.

Sorg C, Riedl V, Muhlau M, Calhoun VD, Eichele T, Laer L, Drzezga A, Forstl H, Kurz A, Zimmer C, Wohlschlager AM (2007): Selective changes of resting-state networks in individuals at risk for Alzheimer's disease. Proc Natl Acad Sci U S A 104:18760–18765.

Stagg CJ, Best JG, Stephenson MC, O'shea J, Wylezinska M, Kincses ZT, Morris PG, Matthews PM, Johansen-Berg H (2009): Polarity-sensitive modulation of cortical neurotransmitters by transcranial stimulation. J Neurosci 29:5202–5206.

Tomasi D, Ernst T, Caparelli EC, Chang L (2006): Common deactivation patterns during working memory and visual attention tasks: An intra-subject fMRI study at 4 Tesla. Hum Brain Mapp 27:694–705.

Vandermeeren Y, Jamart J, Ossemann M (2010): Effect of tDCS with an extracephalic reference electrode on cardio-respiratory and autonomic functions. BMC Neurosci 11:38.

Williams JA, Imamura M, Fregni F (2009): Updates on the use of non-invasive brain stimulation in physical and rehabilitation medicine. J Rehabil Med 41:305–311.

Zaghi S, Heine N, Fregni F (2009): Brain stimulation for the treatment of pain: A review of costs, clinical effects, and mechanisms of treatment for three different central neuromodulatory approaches. J Pain Manag 2:339–352.